perpendicular to CD. Assume an infinite array of identical ledges of height (BC) = h and spacing (CD) = l.

3.16 Using arguments similar to those used in connection with Fig. 3.68 show that a coherent twin boundary in an fcc metal will not migrate by the random jumping of atoms across the interface. Suggest an interfacial structure that would result in a highly mobile interface (see exercise 3.15).

3.17 What are the most likely atomic processes involved in the migration of (i) solid/vapour interfaces, (ii) solid/liquid interfaces in non-metals, (iii) solid/liquid interfaces in metals.

3.18 By using a similar approach to the derivation of Equation 3.20 for a high-angle grain boundary, show that the net flux of B atoms across the α/β interface in Fig. 3.67 is given by

$$J_B^i = \frac{A_\beta n_\alpha \nu_\alpha}{RT} \exp\left(-\frac{\Delta\mu^a}{RT}\right) \Delta\mu_B^i$$

3.19 Derive Equation 3.53 for an ideal or dilute solution.

3.20 If an alloy containing β precipitates in an α matrix is given a solution treatment by heating to a temperature above the equilibrium β solvus the precipitates will dissolve. (See for example the phase diagram in Fig. 1.36.) Show with diagrams how the composition will change in the vicinity of an α/β interface during dissolution if the dissolution is (i) diffusion controlled, (ii) interface controlled, (iii) under mixed control. Indicate compositions by reference to a phase diagram where appropriate.

4
Solidification

Solidification and melting are transformations between crystallographic and non-crystallographic states of a metal or alloy. These transformations are of course basic to such technological applications as ingot casting, foundry casting, continuous casting, single-crystal growth for semiconductors, directionally solidified composite alloys, and more recently rapidly solidified alloys and glasses. Another important and complex solidification and melting process, often neglected in textbooks on solidification, concerns the process of fusion welding. An understanding of the mechanism of solidification and how it is affected by such parameters as temperature distribution, cooling rate and alloying, is important in the control of mechanical properties of cast metals and fusion welds. It is the objective of this chapter to develop some of the basic concepts of solidification, and apply these to some of the more important practical processes such as ingot casting, continuous casting and fusion welding. We then consider a few practical examples illustrating the casting or welding of engineering alloys in the light of the theoretical introduction.

4.1 Nucleation in Pure Metals

If a liquid is cooled below its equilibrium melting temperature (T_m) there is a driving force for solidification ($G_L - G_S$) and it might be expected that the liquid phase would spontaneously solidify. However, this is not always the case. For example under suitable conditions liquid nickel can be *undercooled* (or *supercooled*) to 250 K below T_m (1453 °C) and held there indefinitely without any transformation occurring. The reason for this behaviour is that the transformation begins by the formation of very small solid particles or *nuclei*. Normally undercoolings as large as 250 K are not observed, since in practice the walls of the liquid container and solid impurity particles in the liquid catalyse the nucleation of solid at undercoolings of only ~1 K. This is known as *heterogeneous* nucleation. The large undercoolings mentioned above are only obtained when no heterogeneous nucleation sites are available, i.e. when solid nuclei must form *homogeneously* from the liquid. Experimentally this can be achieved by dividing the liquid into tiny droplets, many of which remain impurity-free and do not solidify until very large undercoolings are reached[1].

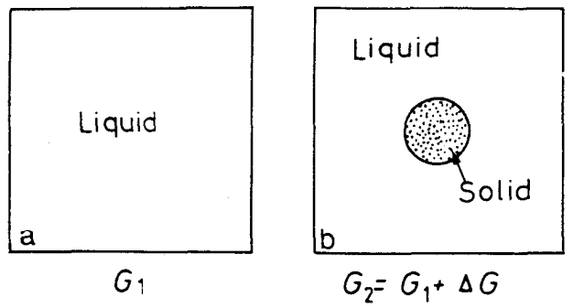

Fig. 4.1 Homogeneous nucleation.

4.1.1 *Homogeneous Nucleation*

Consider a given volume of liquid at a temperature ΔT below T_m with a free energy G_1, Fig. 4.1a. If some of the atoms of the liquid cluster together to form a small sphere of solid, Fig. 4.1b, the free energy of the system will change to G_2 given by:

$$G_2 = V_S G_v^S + V_L G_v^L + A_{SL}\gamma_{SL}$$

where V_S is the volume of the solid sphere, V_L the volume of liquid, A_{SL} is the solid/liquid interfacial area, G_v^S and G_v^L are the free energies per unit volume of solid and liquid respectively, and γ_{SL} the solid/liquid interfacial free energy. The free energy of the system without any solid present is given by

$$G_1 = (V_S + V_L)G_v^L$$

The formation of solid therefore results in a free energy change $\Delta G = G_2 - G_1$ where:

$$\Delta G = -V_S\Delta G_v + A_{SL}\gamma_{SL} \tag{4.1}$$

and

$$\Delta G_v = G_v^L - G_v^S \tag{4.2}$$

For an undercooling ΔT, ΔG_v is given by Equation 1.17 as

$$\Delta G_v = \frac{L_v\Delta T}{T_m} \tag{4.3}$$

where L_v is the latent heat of fusion per unit volume. Below T_m, ΔG_v is positive so that the free energy change associated with the formation of a small volume of solid has a negative contribution due to the lower free energy of a bulk solid, but there is also a positive contribution due to the creation of a solid/liquid interface. The excess free energy associated with the solid particle can be minimized by the correct choice of particle shape. If γ_{SL} is

isotropic this is a sphere of radius r. Equation 4.1 then becomes

$$\Delta G_r = -\frac{4}{3}\pi r^3\Delta G_v + 4\pi r^2\gamma_{SL} \tag{4.4}$$

This is illustrated in Fig. 4.2. Since the interfacial term increases as r^2 whereas the volume free energy released only increases as r^3, the creation of small particles of solid always leads to a free energy increase. It is this increase that is able to maintain the liquid phase in a metastable state almost indefinitely at temperatures below T_m. It can be seen from Fig. 4.2 that for a given undercooling there is a certain radius, r^*, which is associated with a maximum excess free energy. If $r < r^*$ the system can lower its free energy by dissolution of the solid, whereas when $r > r^*$ the free energy of the system decreases if the solid grows. Unstable solid particles with $r < r^*$ are known as clusters or embryos while stable particles with $r > r^*$ are referred to as nuclei—r^* is known as the critical nucleus size. Since $dG = 0$ when $r = r^*$ the critical nucleus is effectively in (unstable) equilibrium with the surrounding liquid.

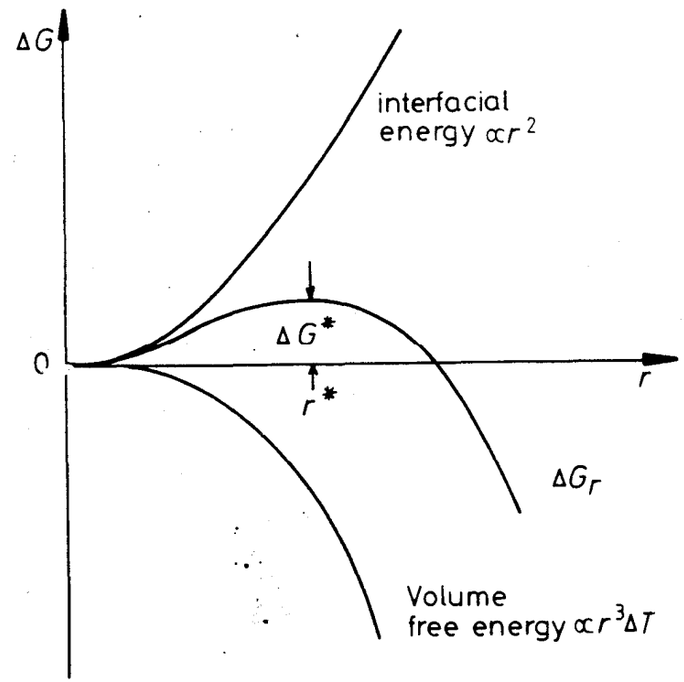

Fig. 4.2 The free energy change associated with homogeneous nucleation of a sphere of radius r.

It can easily be shown by differentiation of Equation 4.4 that

$$r^* = \frac{2\gamma_{SL}}{\Delta G_v} \tag{4.5}$$

and

$$\Delta G^* = \frac{16\pi\gamma_{SL}^3}{3(\Delta G_v)^2} \tag{4.6}$$

Substituting Equation 4.3 for ΔG_v gives

$$r^* = \left(\frac{2\gamma_{SL}T_m}{L_v}\right)\frac{1}{\Delta T} \tag{4.7}$$

and

$$\Delta G^* = \left(\frac{16\pi\gamma_{SL}^3 T_m^2}{3L_v^2}\right)\frac{1}{(\Delta T)^2} \tag{4.8}$$

Note how r^* and ΔG^* decrease with increasing undercooling (ΔT).

Equation 4.5 could also have been obtained from the Gibbs–Thomson equation. Since r^* is the radius of the solid sphere that is in (unstable) equilibrium with the surrounding liquid, the solidified sphere and liquid must then have the same free energy. From Equation 1.58 a solid sphere of radius r will have a free energy greater than that of bulk solid by $2\gamma V_m/r$ per mole or $2\gamma/r$ per unit volume. Therefore it can be seen from Fig. 4.3 that equality of

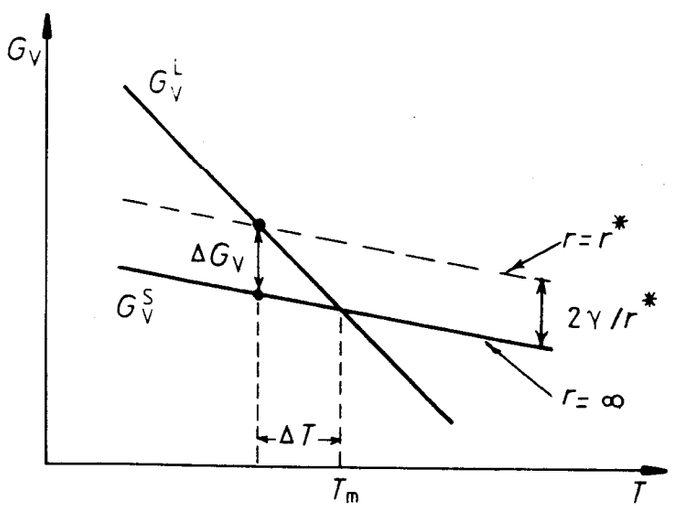

Fig. 4.3 Volume free energy as a function of temperature for solid and liquid phases, showing the origin of ΔG_v and r^*.

free energy implies

$$\Delta G_v = 2\gamma_{SL}/r^* \tag{4.9}$$

which is identical to Equation 4.5.

To understand how it is possible for a stable solid nucleus to form homogeneously from the liquid it is first necessary to examine the atomic structure of the liquid phase. From dilatometric measurements it is known that at the melting point the liquid phase has a volume 2–4% greater than the solid. Therefore there is a great deal more freedom of movement of atoms in the liquid and when averaged over a period of time the atom positions appear completely random. However, an instantaneous picture of the liquid would reveal the presence of many small close-packed clusters of atoms which are temporarily in the same crystalline array as in the solid, Fig. 4.4. On average the number of spherical clusters of radius r is given by

$$n_r = n_0 \exp\left(-\frac{\Delta G_r}{kT}\right) \tag{4.10}$$

where n_0 is the total number of atoms in the system, ΔG_r is the excess free energy associated with the cluster, Equation 4.4, and k is Boltzmann's constant. For a liquid above T_m this relationship applies for all values of r. Below T_m it only applies for $r \leq r^*$ because clusters greater than the critical size are stable nuclei of solid and no longer part of the liquid. Since n_r decreases exponentially with ΔG_r (which itself increases rapidly with r) the probability of finding a given cluster decreases very rapidly as the cluster size increases. For example by combining Equations 4.4 and 4.10 it can be shown (exercise 4.2) that 1 mm^3 of copper at its melting point ($\sim 10^{20}$ atoms) should on average contain $\sim 10^{14}$ clusters of 0.3 nm radius (i.e. ~10 atoms) but only ~10 clusters with a radius of 0.6 nm (i.e. ~60 atoms). These numbers are of course only approximate. Such small clusters of atoms cannot be considered to be spherical, and even more important the effective value of γ used in calculating ΔG_r (equation 4.4) is very probably a function of the cluster size. However the above calculations do illustrate how sensitively cluster density depends on their size. Also, it can be seen that there is effectively a maximum

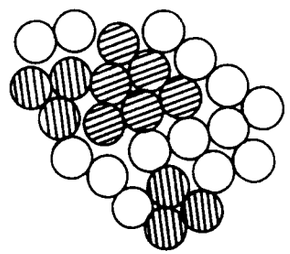

Fig. 4.4 A two-dimensional representation of an instantaneous picture of the liquid structure. Many close-packed crystal-like clusters (shaded) are present.

cluster size, ~100 atoms, which has a reasonable probability of occurring in the liquid. The same sort of calculations can be made at temperatures other than T_m. Below T_m there is an increasing contribution from ΔG_v in Equation 4.4 as the solid becomes progressively more stable and this has the effect of increasing the 'maximum' cluster size somewhat. Figure 4.5 shows schematically how r_{max} varies with ΔT. Of course larger clusters than r_{max} are possible in large enough systems or given sufficient time, but the probability of finding clusters only slightly larger than r_{max} is extremely small.

The critical nucleus size r^* is also shown in Fig. 4.5. It can be seen that at small undercoolings, r^* is so large that there will be virtually no chance of forming a stable nucleus. But as ΔT increases r^* and ΔG^* decrease, and for supercoolings of ΔT_N or greater there is a very good chance of some clusters reaching r^* and growing into stable solid particles. In the small droplet experiment, therefore, homogeneous nucleation should occur when the liquid is undercooled by $\sim\Delta T_N$.

The same conclusion can also be reached by an energy approach. The creation of a critical nucleus can be considered to be a thermally activated process, i.e. a solid-like cluster must be able to cross the nucleation barrier ΔG^* before it becomes a stable nucleus. Since the probability of achieving this energy is proportional to $\exp(-\Delta G^*/kT)$ nucleation will only become possible when ΔG^* is reduced below some critical value which can be shown to be $\sim 78\ kT$ (see below).

4.1.2 *The Homogeneous Nucleation Rate*

Let us consider how fast solid nuclei will appear in the liquid at a given undercooling. If the liquid contains C_0 atoms per unit volume, the number of

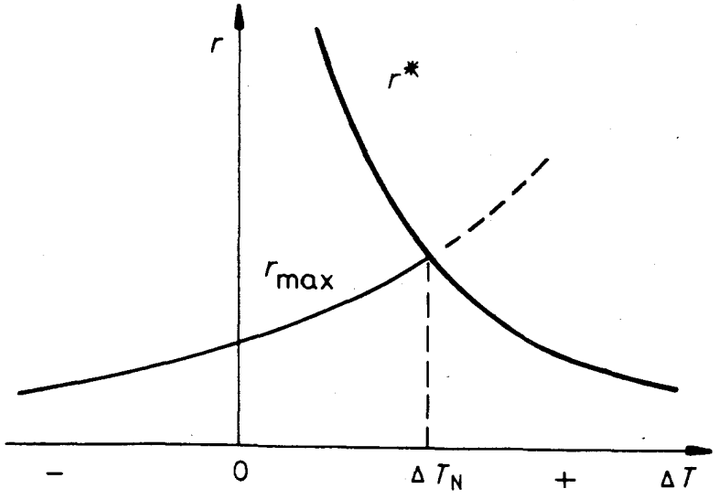

Fig. 4.5 The variation of r^* and r_{max} with undercooling ΔT.

clusters that have reached the critical size (C^*) can be obtained from Equation 4.10 as

$$C^* = C_0 \exp\left(-\frac{\Delta G^*_{hom}}{kT}\right) \quad \text{clusters m}^{-3} \tag{4.11}$$

The addition of one more atom to each of these clusters will convert them into stable nuclei and, if this happens with a frequency f_0, the homogeneous nucleation rate will be given by

$$N_{hom} = f_0 C_0 \exp\left(-\frac{\Delta G^*_{hom}}{kT}\right) \quad \text{nuclei m}^{-3}\ \text{s}^{-1} \tag{4.12}$$

where f_0 is a complex function that depends on the vibration frequency of the atoms, the activation energy for diffusion in the liquid, and the surface area of the critical nuclei. Its exact nature is not important here and it is sufficient to consider it a constant equal to $\sim 10^{11}$.* Since C_0 is typically $\sim 10^{29}$ atoms m^{-3} a reasonable nucleation rate (1 cm^{-3} s^{-1}) is obtained when $\Delta G^* \sim 78\ kT$.

$$N_{hom} = f_0 C_0 \exp\left\{-\frac{A}{(\Delta T)^2}\right\} \tag{4.13}$$

where A is relatively insensitive to temperature and is given by

$$A = \frac{16\pi\gamma_{SL}^3 T_m^2}{3L_v^2 kT}$$

N_{hom} is plotted as a function of ΔT in Fig. 4.6. As a result of the $(\Delta T)^2$ term, inside the exponential N_{hom} changes by orders of magnitude from essentially zero to very high values over a very narrow temperature range, i.e. there is effectively a critical undercooling for nucleation ΔT_N. This is the same as ΔT_N in Fig. 4.5, but Fig. 4.6 demonstrates more vividly how virtually no nuclei are formed until ΔT_N is reached after which there is an 'explosion' of nuclei.

The small droplet experiments of Turnbull *et al.*[1] have shown that ΔT_N is ~0.2 T_m for most metals (i.e. ~200 K). The measured values of ΔT_N have in fact been used along with Equation 4.13 to derive the values of interfacial free energy given in Table 3.4.

In practice homogeneous nucleation is rarely encountered in solidification.

* Since atomic jumps from the liquid on to the cluster are thermally activated, f_0 will in fact diminish with decreasing temperature. In some metallic systems the liquid can be rapidly cooled to temperatures below the so-called glass transition temperature without the formation of crystalline solid. f_0 is very small at these temperatures and the supercooled liquid is a relatively stable metallic glass or amorphous metal. The variation of f_0 with temperature is very important with solid-state transformations, and it is covered in Chapter 5. For further details on alloys rapidly quenched from the melt see R.W. Cahn and P. Haasen (Eds), *Physical Metallurgy*, North-Holland, 1983, Chapter 28.

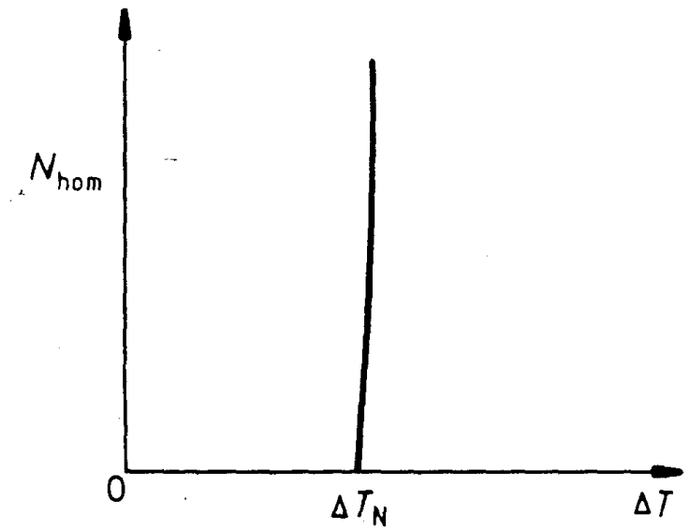

Fig. 4.6 The homogeneous nucleation rate as a function of undercooling ΔT. ΔT_N is the critical undercooling for homogeneous nucleation.

Instead heterogeneous nucleation occurs at crevices in mould walls, or at inpurity particles suspended in the liquid.

4.1.3 *Heterogeneous Nucleation*

From the expression for ΔG^* (Equation 4.8) it can be seen that if nucleation is to be made easier at small undercoolings the interfacial energy term must be reduced. A simple way of effectively achieving this is if the nucleus forms in contact with the mould wall. Consider a solid embryo forming in contact with a perfectly flat mould wall as depicted in Fig. 4.7. Assuming γ_{SL} is isotropic it can be shown that for a given volume of solid the total interfacial energy of the system is minimized if the embryo has the shape of a spherical

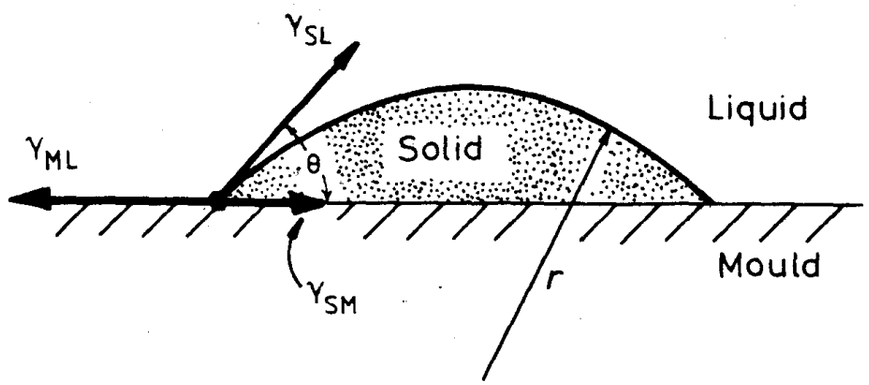

Fig. 4.7 Heterogeneous nucleation of spherical cap on a flat mould wall.

cap with a 'wetting' angle θ given by the condition that the interfacial tensions γ_{ML}, γ_{SM} and γ_{SL} balance in the plane of the mould wall.

$$\gamma_{ML} = \gamma_{SM} + \gamma_{SL} \cos \theta$$

or

$$\cos \theta = (\gamma_{ML} - \gamma_{SM})/\gamma_{SL} \tag{4.14}$$

Note that the vertical component of γ_{SL} remains unbalanced. Given time this force would pull the mould surface upwards until the surface tension forces balance in all directions. Therefore Equation 4.14 only gives the optimum embryo shape on the condition that the mould walls remain planar.

The formation of such an embryo will be associated with an excess free energy given by

$$\Delta G_{het} = -V_S \Delta G_v + A_{SL}\gamma_{SL} + A_{SM}\gamma_{SM} - A_{SM}\gamma_{ML} \tag{4.15}$$

where V_S is the volume of the spherical cap, A_{SL} and A_{SM} are the areas of the solid/liquid and solid/mould interfaces, and γ_{SL}, γ_{SM} and γ_{ML} are the free energies of the solid/liquid, solid/mould and mould/liquid interfaces. Note that there are now three interfacial energy contributions. The first two are positive as they arise from interfaces created during the nucleation process. The third, however, is due to the destruction of the mould/liquid interface under the spherical cap and resuits in a negative energy contribution.

It can be easily shown (see exercise 4.6) that the above equation can be written in terms of the wetting angle (θ) and the cap radius (r) as

$$\Delta G_{het} = \left\{ -\frac{4}{3}\pi r^3 \Delta G_v + 4\pi r^2 \gamma_{SL} \right\} S(\theta) \tag{4.16}$$

where

$$S(\theta) = (2 + \cos \theta)(1 - \cos \theta)^2/4 \tag{4.17}$$

Note that except for factor $S(\theta)$ this expression is the same as that obtained for homogeneous nucleation, Equation 4.4. $S(\theta)$ has a numerical value ≤ 1 dependent only on θ, i.e. the shape of the nucleus. It is therefore referred to as a shape factor. ΔG_{het} is shown in Fig. 4.8 along with ΔG_{hom} for comparison. By differentiation of Equation 4.16 it can be shown that

$$r^* = \frac{2\gamma_{SL}}{\Delta G_v} \tag{4.18}$$

and

$$\Delta G^* = \frac{16\pi\gamma_{SL}^3}{3\Delta G_v^2} \cdot S(\theta) \tag{4.19}$$

Therefore the activation energy barrier against heterogeneous nucleation (ΔG^*_{het}) is smaller than ΔG^*_{hom} by the shape factor $S(\theta)$. In addition the critical

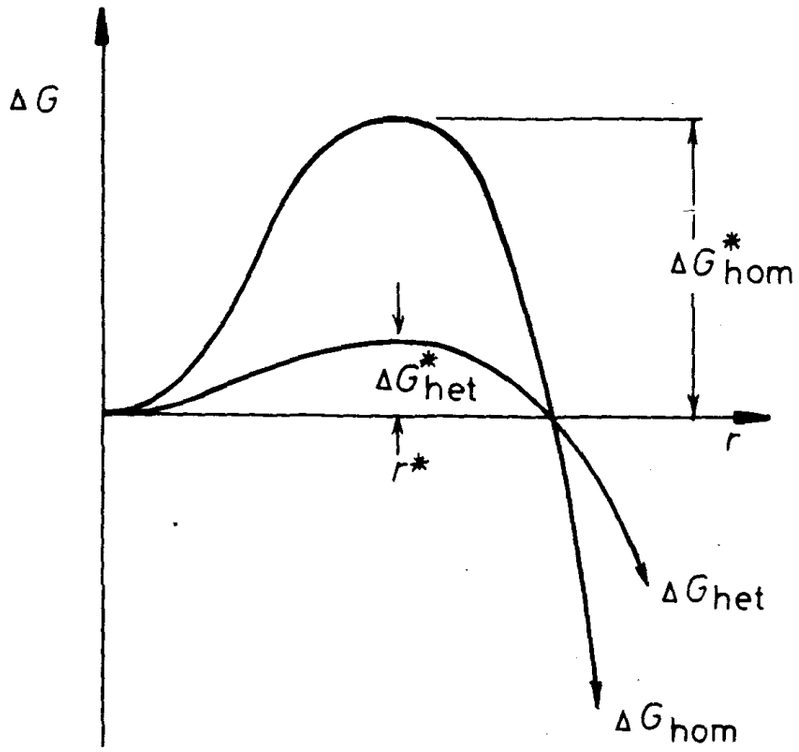

Fig. 4.8 The excess free energy of solid clusters for homogeneous and heterogeneous nucleation. Note r^* is independent of the nucleation site.

nucleus radius (r^*) is unaffected by the mould wall and only depends on the undercooling. This result was to be expected since equilibrium across the curved interface is unaffected by the presence of the mould wall.

Combining Equations 4.6 and 4.19 gives

$$\Delta G^*_{het} = S(\theta)\Delta G^*_{hom} \tag{4.20}$$

If for example $\theta = 10°$, $S(\theta) \sim 10^{-4}$, i.e. the energy barrier for heterogeneous nucleation can be very much smaller than for homogeneous nucleation. Significant reductions are also obtained for higher values of θ, e.g. when $\theta = 30°$, $S = 0.02$; even when $\theta = 90°$, $S = 0.5$. It should be noted that the above model breaks down for $\theta = 0$. In this case the nucleus must be modelled in some other way, e.g. as shown in Fig. 4.12.

The effect of undercooling on ΔG^*_{het} and ΔG^*_{hom} is shown schematically in Fig. 4.9. If there are n_1 atoms in contact with the mould wall the number of nuclei should be given by

$$n^* = n_1 \exp\left(-\frac{\Delta G^*_{het}}{kT}\right). \tag{4.21}$$

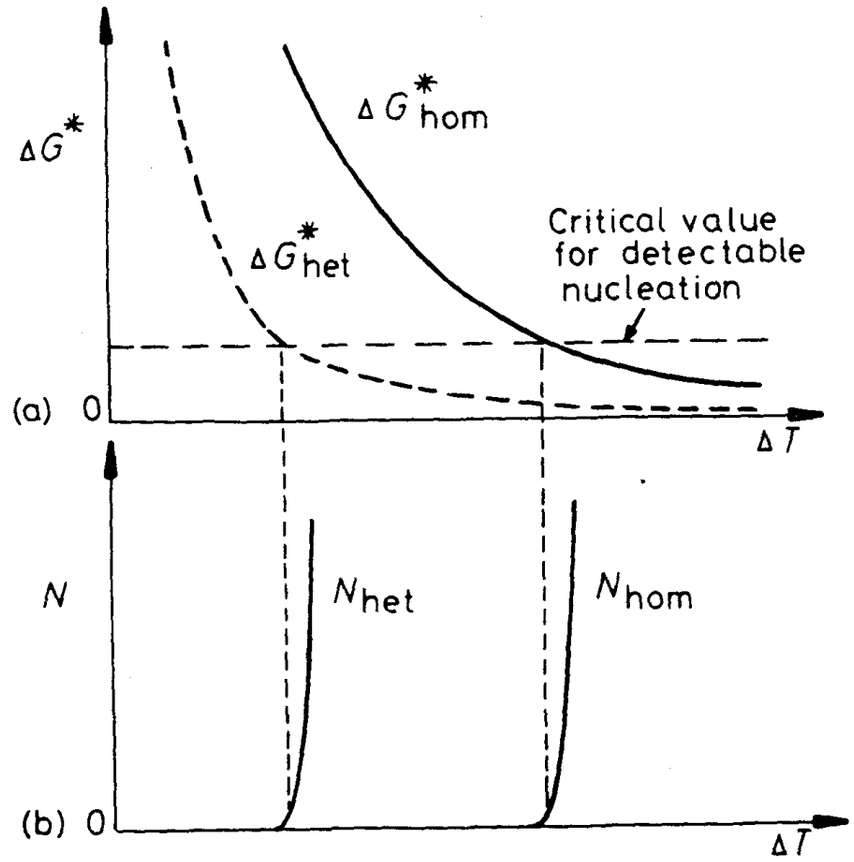

Fig. 4.9 (a) Variation of ΔG^* with undercooling (ΔT) for homogeneous and heterogeneous nucleation. (b) The corresponding nucleation rates assuming the same critical value of ΔG^*.

Therefore heterogeneous nucleation should become feasible when ΔG^*_{het} becomes sufficiently small. The critical value for ΔG^*_{het} should not be very different from the critical value for homogeneous nucleation. It will mainly depend on the magnitude of n_1 in the above equation. Assuming for the sake of simplicity that the critical value is again $\sim 78\,kT$ it can be seen from Fig. 4.9 that heterogeneous nucleation will be possible at much lower undercoolings than are necessary for homogeneous nucleation.

To be more precise, the *volume* rate of heterogeneous nucleation ought to be given by an equation of the form

$$N_{het} = f_1 C_1 \exp\left(-\frac{\Delta G^*_{het}}{kT}\right) \tag{4.22}$$

where f_1 is a frequency factor similar to f_0 in Equation 4.12, C_1 is the number of atoms in contact with heterogeneous nucleation sites per unit volume of liquid.